Indirect transmission and the effect of seasonal pathogen inactivation on infectious disease periodicity

Marguerite Robinson[a,*,1] Yannis Drossinos[a] & Nikolaos I. Stilianakis[a,b].

[a]Joint Research Centre, European Commission, I-21027 Ispra (VA), Italy

[b]Department of Biometry and Epidemiology, University of Erlangen-Nuremberg, Erlangen, Germany

[*]Corresponding author, email: marguerite.robinson@ic3.cat, phone: +34 935679977

Abstract

The annual occurrence of many infectious diseases remains a constant burden to public health systems. The seasonal patterns in respiratory disease incidence observed in temperate regions have been attributed to the impact of environmental conditions on pathogen survival. A model describing the transmission of an infectious disease by means of a pathogenic state capable of surviving in an environmental reservoir outside of its host organism is presented in this paper. The ratio of pathogen lifespan to the duration of the infectious disease state is found to be a critical parameter in determining disease dynamics. The introduction of a seasonally forced pathogen inactivation rate identifies a time delay between peak pathogen survival and peak disease incidence. The delay is dependent on specific disease parameters and, for influenza, decreases with increasing reproduction number. The observed seasonal oscillations are found to have a period identical to that of the seasonally forced inactivation rate and which is independent of the duration of infection acquired immunity.

Keywords influenza, seasonality, indirect transmission, pathogen inactivation

---

[1]Present address: Institut Català de Ciències del Clima (IC³), C/ Doctor Trueta 203, 08005 Barcelona, Spain.

1 Introduction

Many diseases exhibit seasonal cycles in incidence data, most notably childhood diseases such as measles and rubella (Anderson and May, 1991, Dowell, 2001). For such diseases, it is widely accepted that the observed cycles are linked to the timing of school terms and the subsequent increase in contact rates among the immunologically naive child population (Keeling and Rohani, 2001, Stone et al. 2007). The mechanism driving the seasonal occurrence of influenza and other respiratory infections is less well understood. While increased contact rates due to indoor crowding during winter undoubtedly facilitate greater disease transmission, it is more likely a contributing factor and not the driving mechanism (Lofgren et al. 2007). Seasonal influenza places a considerable burden on public health systems with annual global incidence in the range 5 - 15% of the population, resulting in up to 500,000 deaths (Stohr, 2002). Targeted interventions to reduce this burden could be significantly improved if the seasonal stimulus was better understood.

The cause of seasonality must be attributed to annual changes associated with either the host or the infectious disease pathogen (Grassly and Fraser, 2006). In addition to increased contact rates during winter, higher transmission rates have been linked to changes in the human immune system. Possible variations in human immune function have been attributed to fluctuations in melatonin secretion regulated by the annual light-dark cycles and to deficiencies in vitamin D during the winter months (Cannell et al. 2008, Lofgren et al. 2007, Nelson and Demas, 1996). Experiments on mice in an environmentally controlled environment found that mice were more susceptible to infection during the winter months (Schulman and Kilbourne, 1963). For diseases transmitted through indirect pathways (e.g. respiratory droplets, fomites, fungal spores, waterborne pathogens) the ability of the pathogen to survive outside of its host must play a vital role in the transmission process (Grassly and Fraser, 2006). This survival potential would be greatly influenced by environmental factors. Early studies on the survival of the influenza virus in air indicated that pathogen survival peaks at low relative humidity and low temperatures resulting in

increased viral transmission (Harper, 1961, Hemmes et al. 1960). Experiments to study the airborne transmission of influenza among Guinea pigs further supported this theory indicating that transmission among subjects peaked in cold dry air (Lowen et al. 2007). However, while indoor relative humidity is minimized in winter, outdoor humidity peaks. More recent studies identify absolute humidity as a more likely seasonal driver, as both indoor and outdoor absolute humidity display cyclic behavior in temperate regions that minimizes in winter (Shaman and Kohn, 2009). Influenza virus survival increases with low absolute humidity leading to increased transmission in winter (Shaman et al. 2010). Other theories for increased viral inactivation in summer consider ultraviolet radiation and air toxicity, however, little work has been undertaken to support such theories (Weber and Stilianakis, 2008).

A crucial factor to consider when assessing the impact of environmental factors on seasonal transmission is the mode of disease transmission. For respiratory diseases three modes of pathogen transmission have been identified: droplet, contact and airborne transmission (Weber and Stilianakis, 2008). Droplet transmission occurs when, following an expiratory event by an infected individual, large pathogen-carrying droplets (diameter $\gtrsim 10~\mu$m) are deposited directly onto the mucous membranes of a susceptible person. The direct nature of such a transmission pathway precludes a significant impact by environmental factors on either the droplet itself or its pathogen load. Conversely, the contact (through fomites or direct human-to-human contact) and airborne (small aerosol droplets with diameter $\lesssim 10~\mu$m) modes of transmission render the pathogen vulnerable to environmental conditions during prolonged periods spent external to its host organism. For the specific case of the influenza virus, the efficiency of contact transmission is determined by the survival rate of the pathogen on solid surfaces and human skin. The high inactivation rates observed on hands can limit the occurrence of transmission via the contact route, however, a continuous supply of fomites from infected individuals could possibly counteract this (Weber and Stilianakis, 2008). This mode of transmission is greatly influenced by human behavior (e.g. cough etiquette, hand washing) and thus a seasonal variation in its impact would be difficult to quantify. Airborne droplets remain exposed to the ambient environmental conditions for prolonged periods of

time and could act as an important agent driving seasonal disease incidence. For respiratory diseases mediated by airborne droplets and for a spatially homogeneous distribution of susceptibles, pathogen removal is the result of three distinct processes: gravitational settling, pathogen inactivation and inhalation (Stilianakis and Drossinos, 2010). Environmental factors are capable of influencing the first two of these processes (Shaman and Kohn, 2009). The gravitational settling rate of a droplet is determined from its diameter, which is influenced by evaporation effects determined by the ambient air properties. However, a review of experimental studies by Shaman and Kohn (2009) found that there is insufficient evidence to support such a hypothesis. They concluded that seasonal variations in environmental conditions are most likely incorporated through the pathogen inactivation term.

The seasonality of infectious diseases is usually incorporated in deterministic models through a time dependent transmission rate. Outbreaks are typically simulated using a sinusoidal function or, in the case of childhood diseases such as measles, a step function is employed to represent school terms (Grassly and Fraser, 2006, Keeling and Rohani, 2001). Models incorporating natural birth and death processes display damped oscillations towards an endemic disease state (Fisman, 2007). However, if the period of the applied seasonal forcing is close to the intrinsic period of the damped oscillations then the two effects can resonate to produce large amplitude seasonal oscillations (Dushoff et al. 2004). An important consideration in any analysis of seasonal influenza is the process of antigenic drift, whereby continuous small changes in the virus requires the production of a new vaccine each year. This phenomenon can be integrated into the standard deterministic models by allowing recovered individuals to lose their acquired immunity after a specified period of time (Dushoff et al. 2004). An important factor neglected in the standard deterministic models is the mechanism driving the seasonal variation. If the theory that the impact of annual variations in environmental conditions on pathogen survival/inactivation is indeed valid then models should incorporate this phenomenon. In this paper, we present such a model.

In Section 2 we analyze a model for the spread of an infectious disease by means of an

4

intermediate free-living pathogenic state, which is exposed to the ambient environmental conditions. This general model, applicable to a variety of free-living organisms (e.g. viruses, bacteria, fungi, protozoa), was introduced by Anderson and May (1981) to describe indirect disease transmission between free-living microparasites and their invertebrate hosts. Variations of the basic model have been employed to describe the spread of a pathogen through a generalized environmental state (Li et al. 2009), the spread of a waterborne bacteria (Tien and Earn, 2010), bacterial and prion disease in livestock and wildlife (Nieuwhof 2009, Miller 2006), and the transmission of respiratory diseases by airborne droplets (Stilianakis and Drossinos, 2010). The model has even been adapted to describe the spread of fungal spores in a vineyard (Burie, 2006) and the point release of an infectious agent (Reluga, 2004). With such a wide range of applications and descriptive abilities the intrinsic characteristics of the infectious agent are a vital model component and can radically impact the dynamics. A pathogen characteristic of primary importance is its ability to survive for prolonged periods outside of its host, which is directly influenced by environmental conditions and, thus, cannot be ignored in the quest to identify seasonal disease drivers. Therefore, we first analyse the general model and consider its behavior for both short-lived and long-lived pathogenic states. An important outcome of this analysis is that, in the case of short-lived pathogens, a quasi-steady state exists whereby the pathogen dynamics can be described in terms of the infected population alone. This quasi-steady approximation can also be applied to an autonomous model describing seasonal outbreaks. This model is analysed in Section 3, where we consider the consequences of a seasonal variation in the pathogen inactivation rate and how it impacts disease incidence.

2   A model for indirect transmission of an infectious disease

Many infectious diseases are primarily transmitted by means of an intermediate environmental reservoir, in which free-living pathogens are capable of surviving outside of the host

organism. For example, waterborne outbreaks can persist through the shedding of pathogens by an infected individual into a water source which is then ingested by a susceptible individual. Similarly, respiratory diseases can be transmitted from person to person via pathogen loaded airborne droplets or fomites expelled into the environment by infected individuals during expiratory events (e.g. coughing or sneezing). The efficiency of such transmission pathways will depend on the ability of the pathogen to survive in the intermediate reservoir (e.g. air, water). In this section we present a generalized model for the transmission of an infection by means of such a pathogen reservoir.

Consider a closed population of N individuals, of which $S(t)$ are susceptible, $I(t)$ are infected and $R(t)$ are recovered. Infected individuals shed pathogens into an intermediate reservoir, which are free-living (outside of the host organism) and can transmit infection through contact with the susceptible population, Figure 1. The total number of pathogens in the reservoir is $P(t)$. A deterministic model for the disease dynamics is

$$
\begin{aligned}
\frac{dS}{dt} &= d(N - S) + \sigma(N - S - I) - \frac{\beta}{N}PS, \\
\frac{dI}{dt} &= \frac{\beta}{N}PS - (\mu + d)I, \\
\frac{dP}{dt} &= \kappa I - \alpha P,
\end{aligned}
$$

where the total human population $N = S + I + R$ is constant. The duration of time spent in the infected state is $T_I = 1/(\mu + d)$, where $1/\mu$ is the average infectious disease period and $1/d$ is a typical human lifespan. Infected individuals generate pathogens, with a lifespan of $T_P = 1/\alpha$, at a rate κ. Infection acquired immunity is lost after a time period of $1/\sigma$, with $\sigma = 0$ if immunity is permanent. The transmission rate per pathogen is β, determined from the contact rate of a susceptible with a pathogen and the probability of such a contact causing infection. The equation describing pathogen dynamics assumes that pathogen numbers decrease exponentially for positive α. This could be modified to describe pathogens with more complicated life cycles. The pathogen removal rate α can be a complicated function of environmental factors, depending on the specific pathogen type and reservoir characteristics,
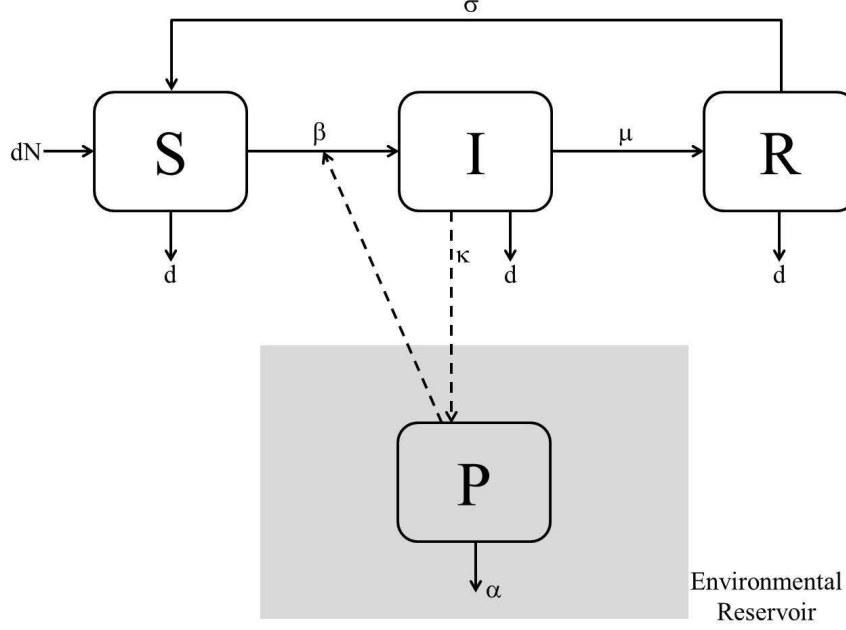
Figure 1: Infection pathway for the transmission of a disease by a free-living pathogen P in a population of susceptible S, infected I and recovered R individuals.

but for now we assume it is constant.

The general model presented here is applicable to a wide variety of diseases such as cholera and influenza in humans (Tien and Earn 2010, Stilianakis and Drossinos 2010) and footrot and chronic wasting disease in animals (Nieuwhof 2009, Miller 2006). In the case of waterborne pathogens, this model has been expanded, specifically in the case of cholera, to include dose dependent infection rates (Codeço 2001, Bertuzzo 2010) and a minimum infectious dose (Joh, 2009). To analyse the general framework of the basic model we omit such disease dependent complications, but will consider this issue in relation to influenza in Section 3.3.

The model can be written in dimensionless form by scaling

$$S, I \sim N, \quad P \sim \frac{\kappa}{\alpha} N, \quad t \sim \frac{1}{\mu + d}, \tag{1}$$

and the dimensionless system is

$$\frac{dS}{dt} = \phi(1 - S) + \psi(1 - S - I) - R_0 PS, \tag{2}$$

$$\frac{dI}{dt} = R_0 PS - I, \tag{3}$$

$$\rho\frac{dP}{dt} = I - P, \tag{4}$$

where dimensionless numbers are defined as

$$R_0 = \frac{\beta\kappa}{\alpha(\mu + d)}, \qquad \phi = \frac{d}{\mu + d}, \qquad \psi = \frac{\sigma}{\mu + d}, \qquad \rho = \frac{\mu + d}{\alpha} = \frac{T_P}{T_I}.$$

The dimensionless number ρ represents the ratio of the pathogen lifespan to that of an infected individual. The dynamics of the pathogen, satisfying (4), will be determined by the magnitude of ρ. The magnitude of R_0 represents the average number of secondary infections from a primary infection and is typically $O(1)$. Finally, ϕ and ψ determine how quickly the pool of susceptible individuals is repopulated from natural birth or death processes and loss of acquired immunity respectively. Suitable initial conditions are

$$S(0) = S_0, \qquad I(0) = 1 - S_0 = I_0, \qquad P(0) = P_0, \tag{5}$$

where it is assumed that no pre-existing immunity is present in the population, $R(0) = 0$.

The system (2)-(4) has two equilibrium states. A disease-free state $E_0 = (1, 0, 0)$ and an endemic state E_e where

$$E_e = (S_e, I_e, P_e) = \left(\frac{1}{R_0}, \frac{(\phi + \psi)(R_0 - 1)}{R_0(\psi + 1)}, \frac{(\phi + \psi)(R_0 - 1)}{R_0(\psi + 1)}\right), \tag{6}$$

which exists when at least one of ϕ or ψ is nonzero and $R_0 > 1$. It can be easily shown by a linear analysis that the disease-free state is locally stable when $R_0 < 1$ and the initial infection (5) dies out. Conversely, the endemic state is locally stable when $R_0 > 1$ and the initial infection will spread approaching the equilibrium state E_e as $t \to \infty$. The equilibrium

point is a stable focus resulting in damped oscillations towards E_e. As we are interested in the long-term seasonal variation in the endemic state we will assume that $R_0 > 1$ for our purposes.

2.1 Short-lived pathogenic state

If the duration of the infectious disease state is significantly longer than the lifespan of the pathogen, $T_P \ll T_I$, then $\rho \ll 1$. This implies that equation (4) rapidly achieves an equilibrium compared with the rest of the system. We can assume that the left-hand side of equation (4) is approximately zero, $\rho \frac{dP}{dt} = 0$, and employ the approximation

$$P \approx I. \tag{7}$$

The system then reduces to the standard SIRS model

$$\frac{dS}{dt} = \phi(1 - S) + \psi(1 - S - I) - R_0 IS, \tag{8}$$

$$\frac{dI}{dt} = (R_0 S - 1)I, \tag{9}$$

with initial conditions

$$S(0) = S_0, \qquad I(0) = I_0, \qquad P(0) = I_0. \tag{10}$$

The quasi-steady state approximation employed above does not imply that $\frac{dP}{dt} = 0$, since P will change in time according to (7). A closed form solution is not possible for the SIRS system. However, the long term behavior is characterized by two possible equilibrium states. A disease-free state $E_0 = (1, 0)$ and the endemic state E_e where

$$E_e = (S_e, I_e) = \left(\frac{1}{R_0}, \frac{(\phi + \psi)(R_0 - 1)}{R_0(\psi + 1)} \right),$$
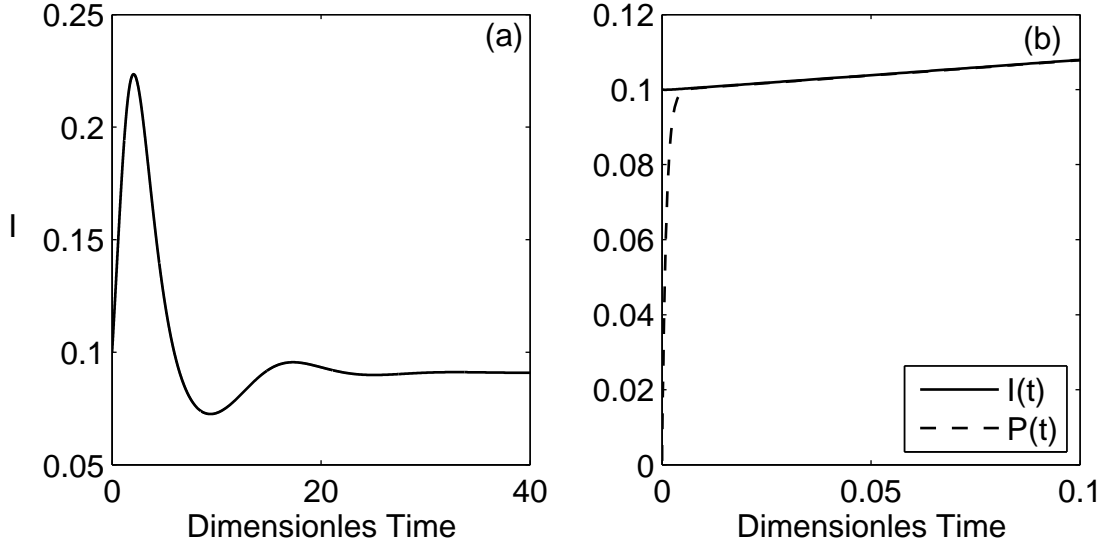
Figure 2: Numerical solution of the SIRS system (8)-(9) with parameter values $\phi = \psi = 0.1$, $R_0 = 2$ and $\rho = 0.001$. Initial conditions are $S(0) = 0.9$, $I(0) = 1 - S(0)$ and $P(0) = 10^{-6}$. (a) Long-time behavior of the infected population (b) Boundary layer region showing the small-time behavior of the infected population and pathogen number.

and $P_e = I_e$ from (7), in agreement with (6). It is trivial to show by a linear analysis that, in the limit $t \to \infty$, the SIRS system approaches this stable endemic state when $R_0 > 1$, which is shown by a numerical solution in Figure 2(a). From (10), the quasi-steady state assumption requires $P(0) = I_0$ and the original initial conditions (5) are not satisfied, except in the unique case where $P_0 = I_0$. This inconsistency arises because the approximation (7) is only valid when $\frac{dP}{dt} \sim O(1)$ and breaks down if P changes rapidly at any point in the domain such that $\rho \frac{dP}{dt}$ is no longer small. There is an initial boundary layer for times of order ρ in which the approximation is invalid and the original scalings (1) are not appropriate, Figure 2(b). In this region $\frac{dP}{dt} \gg 1$ and we rescale the time in equations (2)-(4) using $t = \rho\tau$ to obtain equations for this boundary layer region

$$\frac{dS}{d\tau} = \rho\left[\phi(1 - S) + \psi(1 - S - I) - R_0 PS\right],$$
$$\frac{dI}{d\tau} = \rho\left[R_0 PS - I\right],$$
$$\frac{dP}{d\tau} = I - P.$$

10

At leading order in ρ we then have

$$\frac{dS}{d\tau} = 0, \qquad \frac{dI}{d\tau} = 0, \qquad \frac{dP}{d\tau} = I - P,$$

which has solution

$$S = S_0, \qquad I = I_0, \qquad P = I_0 + (P_0 - I_0)e^{-\tau}.$$

The original initial condition $P(0) = P_0$ is now satisfied and as $\tau \to \infty$ we exit the boundary layer and we have $P \to I_0$ in agreement with the quasi-steady state approximation (10). In theory, unknown constants generated from the solution of the SIRS model in the outer region would be fixed by matching the two solutions in the limits as $t \to 0$ and $\tau \to \infty$. In terms of the long-term behaviour of an infectious disease, we can conclude that the dynamics of the pathogen closely follow those of the infected population and a standard SIRS model is sufficient for a mathematical analysis. However, because the pathogen undergoes rapid changes, the initial transient interval may be important for short-term dynamics.

2.2 Long-lived pathogenic state

If the pathogen survives significantly longer than the duration of the infectious disease state, $T_P \gg T_I$, then $\rho \gg 1$. For convenience, in this section we set $\psi = 0$ so that immunity is permanent. This has the effect of slowing the rate at which the susceptible compartment is repopulated. However, the behavior of the solution is qualitatively similar and the simplified system serves to highlight the primary features. The endemic equilibrium of the full system (2)-(4), with $\psi = 0$, is now given by

$$\tilde{E}_e = (\tilde{S}_e, \tilde{I}_e, \tilde{P}_e) = \left(\frac{1}{R_0}, \frac{\phi(R_0 - 1)}{R_0}, \frac{\phi(R_0 - 1)}{R_0} \right), \tag{11}$$
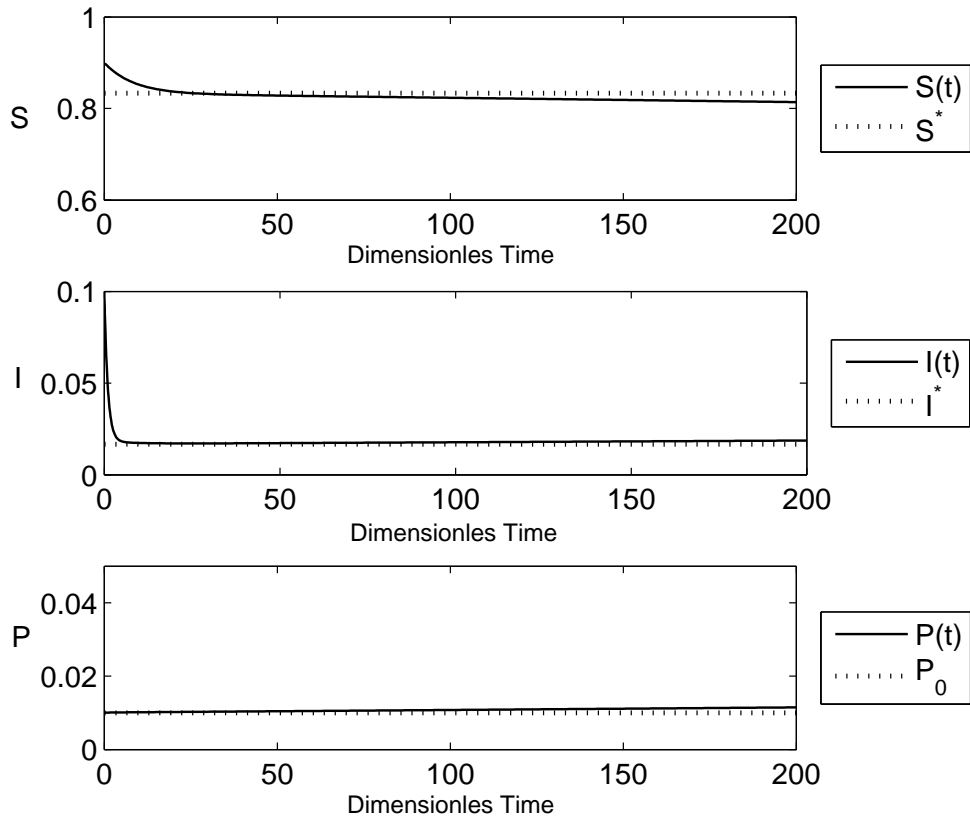
Figure 3: Numerical solution of the system (2)-(4), obtained with initial conditions $S(0) = 0.9$, $I(0) = 0.1$ and $P(0) = 0.01$. Parameter values are $\phi = 0.1$, $\psi = 0$, $R_0 = 2$ and $\rho = 1000$.

and the solution approaches $\tilde{E}_e$ as $t \to \infty$ when $R_0 > 1$. When $\rho \gg 1$ the right-hand side of equation (4) is approximately zero, $(I - P)/\rho \approx 0$, and we can assume that P is in a steady state such that $\frac{dP}{dt} = 0$ and $P = P_0$. The system reduces to

$$\frac{dS}{dt} = \phi(1 - S) - R_0 P_0 S,$$
$$\frac{dI}{dt} = R_0 P_0 S - I,$$

with initial conditions

$$S(0) = S_0, \qquad I(0) = I_0.$$

The linear system is easily solved to obtain

$$S(t) = S^* + (S_0 - S^*)e^{-\frac{\phi}{S^*}t}, \tag{12}$$
$$I(t) = I^* + I^* \frac{S_0 - S^*}{S^* - \phi}(e^{-\frac{\phi}{S^*}t} - e^{-t}) + (I_0 - I^*)e^{-t}, \tag{13}$$

where

$$S^* = \frac{\phi}{\phi + R_0 P_0}, \qquad I^* = R_0 P_0 S^*. \tag{14}$$

The solution of the reduced system clearly satisfies the initial conditions of the full system (5) as $t \to 0$. However, as $t \to \infty$ the solution does not approach the endemic equilibrium (11). At relatively large times, the solution approaches an alternative endemic state $E^* = (S^*, I^*, P_0)$, Figure 3. This inconsistency arises because, for times $t \gtrsim O(\rho)$, P is no longer at a steady state and begins to grow towards its $\tilde{E}_e$ value, Figure 4. Under such circumstances the steady state assumption breaks down. To describe this large-time behaviour, we rescale the time $t = \rho\theta$ and the system becomes

$$\frac{1}{\rho}\frac{dS}{d\theta} = \phi(1 - S) - R_0 P_0 S,$$
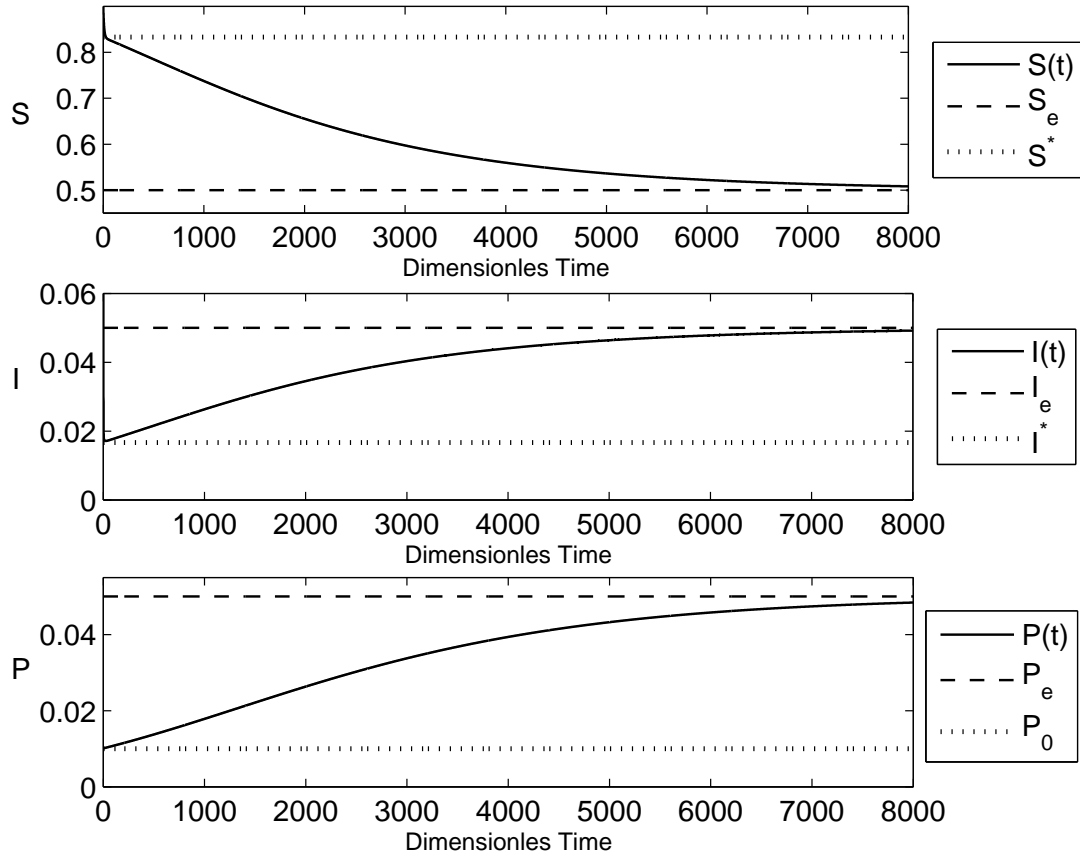$$\frac{1}{\rho}\frac{dI}{d\theta} = R_0 P_0 S - I,$$
$$\frac{dP}{d\theta} = I - P.$$

Figure 4: Numerical solution of the system (2)-(4), obtained with initial conditions $S(0) = 0.9$, $I(0) = 0.1$ and $P(0) = 0.01$. Parameter values are $\phi = 0.1$, $\psi = 0$, $R_0 = 2$ and $\rho = 1000$.

Now, for $\rho \gg 1$ this can be approximated by

$$\phi(1 - S) - R_0 PS = 0,$$

$$R_0 PS - I = 0,$$

$$\frac{dP}{d\theta} = I - P,$$

which has solution

$$S(\theta) = \frac{\phi}{\phi + R_0 P(\theta)}, \qquad I(\theta) = \frac{\phi R_0 P(\theta)}{\phi + R_0 P(\theta)}, \tag{15}$$

where $P(\theta)$ satisfies the first-order equation

$$\frac{dP}{d\theta} = \frac{\phi R_0 P(\theta)}{\phi + R_0 P(\theta)} - P(\theta). \tag{16}$$

For this large time solution to match the inner one, (12)-(13), we require

$$S(\theta \to 0) = S^*, \qquad I(\theta \to 0) = I^*, \qquad P(\theta \to 0) = P_0.$$

which yields

$$S(\theta = 0) = \frac{\phi}{\phi + R_0 P_0}, \qquad I(\theta = 0) = \frac{\phi R_0 P_0}{\phi + R_0 P_0},$$

in agreement with (14). Equation (16) cannot be solved explicitly for $P(\theta)$, however, an implicit solution can be obtained

$$\frac{P_0}{P} \left(\frac{\phi + R_0 P - \phi R_0}{\phi + R_0 P_0 - \phi R_0} \right)^{R_0} = e^{-\theta(R_0 - 1)}.$$

Now, as $\theta \to \infty$ we find that the limiting value of $P(\theta)$, which we denote as P_∞, must satisfy

$$\left(\frac{\phi + R_0 P_\infty - \phi R_0}{\phi + R_0 P_0 - \phi R_0} \right)^{R_0} = 0,$$

which yields

$$P_\infty = \frac{\phi(R_0 - 1)}{R_0} = \tilde{P}_e.$$

15

It follows immediately from (15) that $S \to \tilde{S}_e$ and $I \to \tilde{I}_e$ as $\theta \to \infty$ and the large time solution approaches the endemic equilibrium (11) as required, Figure 4.

2.3 Applications of the model

The model can be used to describe the airborne spread of a respiratory disease by aerosol droplets. The total number of airborne pathogens is $P(t) = N_p D(t)$, where $D(t)$ is the total number of droplets with active pathogens and N_p is the number of pathogens per droplet at the time of expulsion (Stilianakis and Drossinos, 2010). The lifespan of droplets is identical to that of pathogens ($T_P = T_D = 1/\alpha$) as droplets and pathogens are removed by identical processes since they are intrinsically linked. Gravitational settling removes droplets from the environment, which invariably results in the removal of the droplet's pathogen load. Similarly, the inhalation of a droplet by a population member removes pathogens, however, this process had little impact on droplet numbers and can be neglected (Robinson et al. 2012). In addition, a droplet is removed from the infection pathway through pathogen inactivation (i.e. an airborne droplet carrying inactivated pathogens cannot cause infection). The dimensional system describing the infection dynamics is

$$
\begin{aligned}
\frac{dS}{dt} &= d(N - S) + \sigma(N - S - I) - \frac{\beta_d}{N}DS, \\
\frac{dI}{dt} &= \frac{\beta_d}{N}DS - (\mu + d)I, \\
\frac{dD}{dt} &= \kappa_d I - \alpha D,
\end{aligned}
$$

where $\beta_d = \beta N_p$ and $\kappa_d = \frac{\kappa}{N_p}$ are the *droplet* transmission and generation rates respectively. Scaling $D \sim \frac{\kappa_d}{\alpha} N$, the dimensionless system is

$$
\frac{dS}{dt} = \phi(1 - S) + \psi(1 - S - I) - R_0 DS, \tag{17}
$$

$$
\frac{dI}{dt} = R_0 DS - I, \tag{18}
$$

$$
\rho\frac{dD}{dt} = I - D, \tag{19}
$$

16

where all other scales and dimensionless numbers are defined as before. For the particular case of influenza the infectious period is approximately 5 days, $\mu = 0.2$/day, and an average human lifespan is 70 years, $d = 4 \times 10^{-5}$/day. Airborne droplets (of diameter 4 μm) are removed, through the processes of gravitational settling and pathogen inactivation, at a rate of $\alpha = 37.44$/day (Robinson et al. 2012). The droplet generation rate κ_d is based on the number of pathogen loaded droplets emitted during a cough. Generation rates per cough are taken as 160/day (Nicas et al. 2005). The daily generation rate is then obtained by considering a 200-fold increase for a sneeze (Nicas et al. 2005) and a total of 11 sneezes and 360 coughs per day (Atkinson and Wein, 2008), which yields $\kappa_d = 4.1 \times 10^5$/day. Loss of immunity is typically associated with the emergence of new viral strains, with previously infected individuals reverting to a susceptible state after approximately 5 years, $\sigma = 5.5 \times 10^{-4}$/day (Truscott et al. 2012).

For an epidemic in progress the basic reproduction number is typically estimated from incidence data and can vary significantly between different pandemic and seasonal outbreaks. Estimates for the 2009 H1N1 pandemic are in the range $1.3 - 1.7$ (Yang et al. 2009) and an average seasonal value is approximately 1.3 (Chowell et al. 2008). However, we have developed an explicit expression for the transmission rate per droplet β_d which allows a direct estimation of the reproduction number. Firstly, it is important to note that the infectious agent is not the droplet but the pathogens it carries. Therefore, the transmission rate per droplet β_d will depend the transmission rate per pathogen, $\beta_d = \beta_p q_d N_p$, where q_d is the probability of deposition in the human respiratory tract. The minimum infectious dose required to transmit the infection is thus implicitly incorporated into the transmission rate. The transmission rate per pathogen β_p is determined from the contact rate c_d of a susceptible with a droplet and the probability p_d that such a contact will result in successful transmission $\beta_p = c_d p_d$. To derive the contact rate with a droplet it is assumed that each infected person is surrounded by a droplet cloud with volume V_{cl}. It is further assumed that a susceptible individual comes in contact with a droplet through breathing during an encounter with this droplet cloud. If the average breathing rate is B and τ_{ct} is a characteristic time

17

parameter		value
c	contact rate	13 per day
ρ_p	pathogen concentration in the lung fluid	3.71×10^6 pathogens cm^{-3}
B	breathing rate	24 m^3 per day
V_{cl}	personal-cloud volume of an infected person	8 m^3
p_d	infection probability by an inhaled pathogen	0.052
τ_{ct}	characteristic breathing (contact) time	20 min
V_d	pre-evaporation (spherical) droplet volume	2.68×10^{-10} cm^3
q_d	inhaled droplet deposition probability	0.88

Table 1: Parameter values used to determine the transmission rate per droplet.

of breathing during the encounter then the contact rate c_d can be expressed as $c_d = c\frac{B}{V_{cl}}\tau_{ct}$, where c is the average number of total contacts a susceptible individual has per unit time. The transmission rate per droplet is thus

$$\beta_d = c\frac{B}{V_{cl}}\tau_{ct}p_dq_dN_p,$$

and the number of pathogens per droplet can be determined by $N_p = V_d\rho_p$, where V_d is the volume of the (spherical) pre-evaporative droplet and ρ_p is the pathogen concentration of the lung fluid. All the relevant parameter values for influenza are discussed by Stilianakis and Drossinos (2010), and the corresponding values for a 4μm droplet are summarized in Table 1. The transmission rate per pathogen can now be calculated as 0.028/day and the transmission rate per droplet then evaluates to $\beta_d = 2.45 \times 10^{-5}$/day. Finally, the basic reproduction number can be estimated as $R_0 \approx 1.3$, in agreement with seasonal estimates from the literature. Using the parameter values discussed above the dimensionless numbers are estimated as

$$R_0 = 1.3, \qquad \rho \approx 0.005, \qquad \phi \approx 0.0002, \qquad \psi \approx 0.003. \tag{20}$$

The lifespan of droplets (and pathogens) is much less than that of an infected person such that $\rho \ll 1$. Also, for influenza, $\phi \ll \psi \ll 1$ and the repopulation of the susceptible class following an outbreak is a slow process, primarily driven by loss of immunity and not natural births. The numerical solution approaches the endemic equilibrium with damped
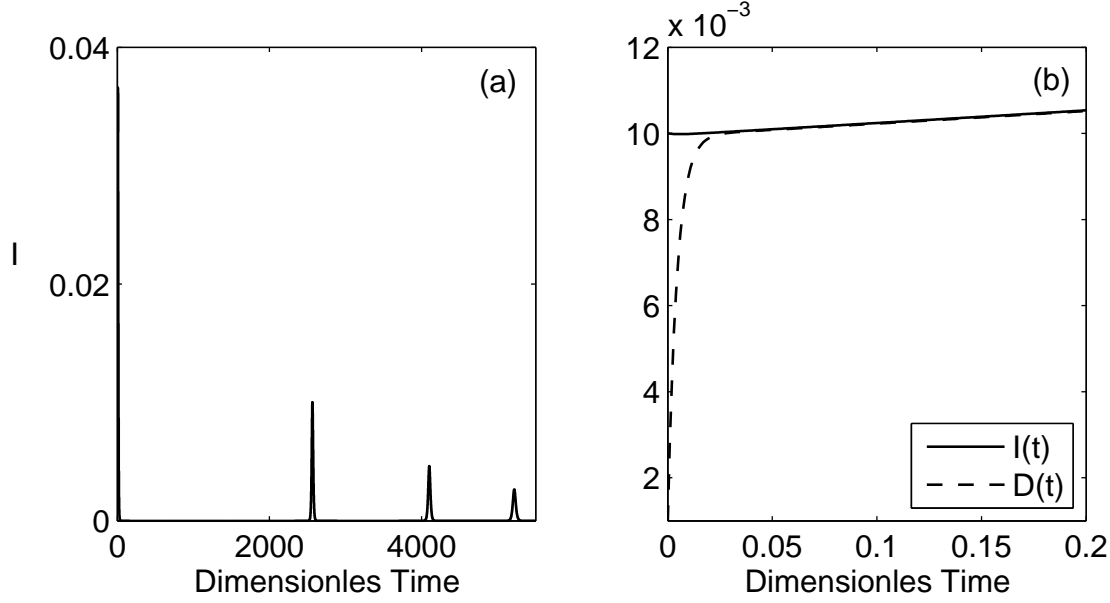
Figure 5: Numerical solution of (17)-(19), with initial conditions $S(0) = 0.99$, $I(0) = 0.01$ and $D(0) = 10^{-3}$. Parameter values for influenza are $R_0 = 1.3$, $\rho \approx 0.005$, $\phi \approx 0.0002$ and $\psi \approx 0.003$.

oscillations of large period ~ 10 years, Figure 5(a). The magnitude of the period is highly sensitive to the duration of immunity, with much shorter times observed between outbreaks if $1/\sigma$ is reduced. The small-time behavior of the model, where droplets rapidly achieve a balance with the infected population, is shown in Figure 5(b). After approximately 6 hours droplets and infected individuals achieve a balance and droplet dynamics thereafter follow the infected population.

The model can also be used to describe the waterborne route of transmission (Codeço, 2001, Tien and Earn, 2010). An example of a pathogen that causes diarrhoeal disease in humans is the protozoa Cryptosporidium. Large outbreaks of Cryptosporidium due to contaminated drinking water are common (Eisenberg et al. 1998, Glaberman et al. 2002). The variable $P(t)$ will represent the number of oocysts in a water source. This pathogen has been recorded surviving in an aqueous suspension for up to 12 months in cold temperatures $\alpha = 0.003$/day, (Peeters et al. 1989). An infection typically persists for $6 - 9$ days, $\mu = 0.14$/day, with infected individuals shedding up to 10^{5-7} oocysts per gram of faeces (Medema et al. 2009). With an average human faecal production rate of 106 g/day (Cummings et

19

al. 1992), we set $\kappa = 10^7$/day. The magnitude of the transmission rate by the waterborne route (in the absence of direct person-to-person transmission) has been estimated to be in the range $[10^{-11}, 10^{-7}]$ and we take $\beta = 10^{-10}$/day (Eisenberg et al. 1998). No immunity is acquired following infection and, for convenience, we assume that immunity is lost one day after recovery $\sigma = 1$/day. Using these parameter values we estimate dimensionless numbers as

$$R_0 = 2.38, \qquad \rho = 46.7, \qquad \phi = 2.7 \times 10^{-4}, \qquad \psi = 7.1.$$

The long lifespan of the cryptosporidium oocysts yields $\rho \gg 1$. The solution of the model is plotted in Figure 6. An initial rapid period can be observed during which P is approximately constant and S and I rapidly approach an intermediate state $(S^*, I^*) = (0.97, 0.02)$. The observed growth in the susceptible population in this region is an artifact of the choice of initial condition. At large times the solution converges to the endemic state $E_e = (S_e, I_e, P_e) = (0.42, 0.5, 0.5)$.

3   Seasonal variation in pathogen inactivation

In this section we consider the dynamics of the model presented in Section 2 when seasonal forcing is applied to the pathogen inactivation rate. We make no assumption as to the precise source of the forcing, merely that it manifests through increased pathogen survival in winter. We consider the specific case of the airborne transmission of respiratory infections by aerosol droplets, as described in Section 2.3.

3.1   The quasi-steady state

To describe the seasonal cycle of respiratory infectious diseases we consider the effects of applying a seasonal forcing to the droplet model of Section 2.3. The forcing is implemented
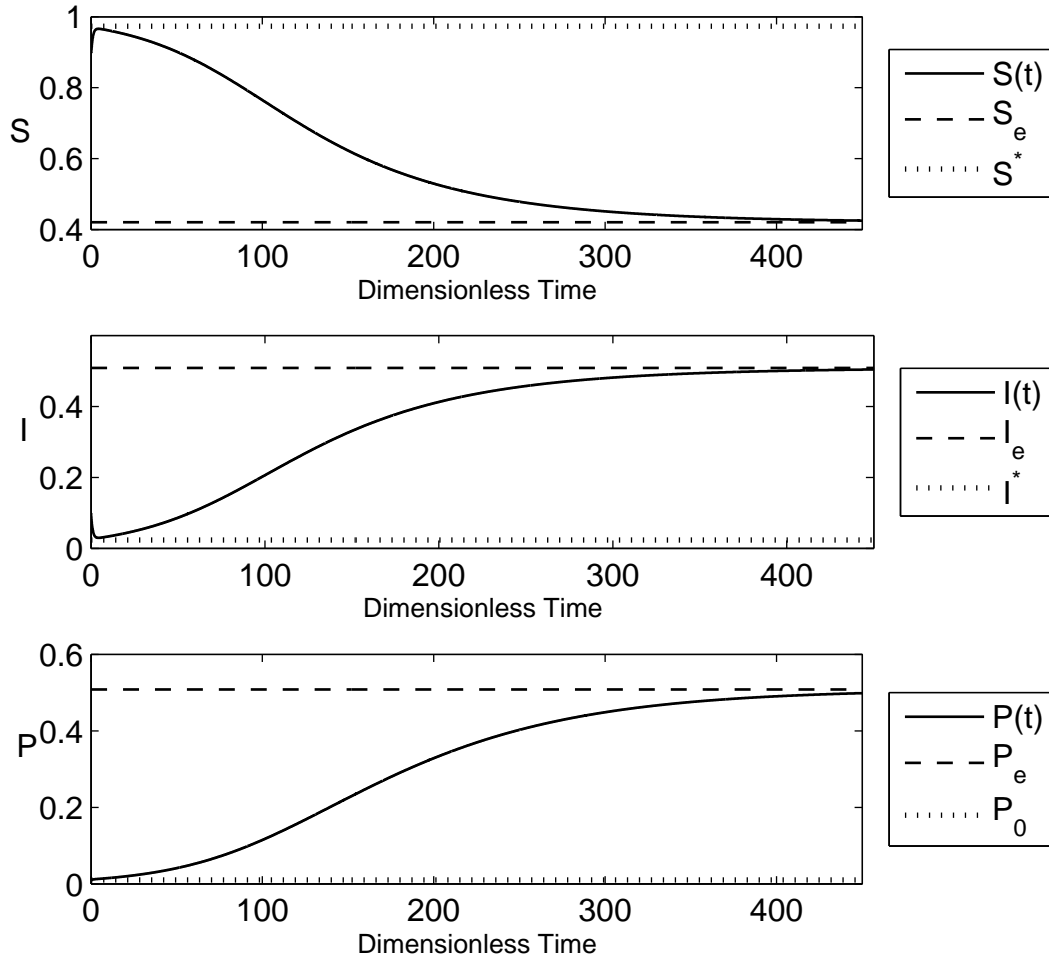
20

Figure 6: Numerical solution of (2)-(4), with initial condition $S(0) = 0.9$, $I(0) = 0.1$ and $P(0) = 0.01$. Parameter values for cryptosporidium are $R_0 = 2.38$, $\rho \approx 46.7$, $\phi \approx 2.7 \times 10^{-4}$ and $\psi \approx 7.1$.

via the droplet removal rate. The dimensional model is

$$\frac{dS}{dt} = d(N - S) + \sigma(N - S - I) - \frac{\beta_d}{N}DS,$$

$$\frac{dI}{dt} = \frac{\beta_d}{N}DS - (\mu + d)I,$$

$$\frac{dD}{dt} = \kappa_d I - \alpha(t)D.$$

We take

$$\alpha = \theta + \eta_0\{1 + \eta_1 \cos(\omega t)\},$$

where ω is the frequency of oscillation of the inactivation rate, θ is the constant rate at which gravity and inhalation remove droplets. The parameter η_0 is the pathogen inactivation rate in the absence of seasonal forcing and η_1 represents the amplitude of the applied forcing term. For convenience, we denote $\alpha_0 = \theta + \eta_0$. We nondimensionalise by scaling

$$S, I \sim N, \quad D \sim \frac{\kappa_d}{\alpha_0}N, \quad \alpha \sim \alpha_0, \quad t \sim \frac{1}{\mu + d},$$

and we can write the dimensionless system as

$$\frac{dS}{dt} = \phi(1 - S) + \psi(1 - S - I) - R_0 DS, \tag{21}$$

$$\frac{dI}{dt} = R_0 DS - I, \tag{22}$$

$$\rho\frac{dD}{dt} = I - \alpha D, \tag{23}$$

$$\alpha = 1 + \alpha_1 \cos(\Omega t), \tag{24}$$

where dimensionless numbers are defined as

$$R_0 = \frac{\beta_d \kappa_d}{\alpha_0(\mu + d)}, \quad \phi = \frac{d}{\mu + d}, \quad \psi = \frac{\sigma}{\mu + d}, \quad \rho = \frac{\mu + d}{\alpha_0} = \frac{T_D}{T_I}, \quad \alpha_1 = \frac{\eta_0 \eta_1}{\alpha_0}, \quad \Omega = \frac{\omega}{\mu + d}. \tag{25}$$

In the absence of seasonal forcing ($\alpha_1 \equiv 0$) the long-term behaviour is characterized by an endemic equilibrium state given by

$$S_e = \frac{1}{R_0}, \qquad I_e = D_e = \frac{(\phi + \psi)(R_0 - 1)}{R_0(\psi + 1)},$$

in agreement with (6) where $\alpha = \alpha_0$. This equilibrium exists and is stable when $R_0 > 1$ and one of either ϕ or ψ are nonzero, enabling the repopulation of the susceptible compartment.

The lifespan of airborne respiratory pathogens is relatively small, as gravity and pathogen inactivation invariably remove the pathogen-loaded droplets on a timescale significantly shorter than the infectious period, $T_D \ll T_I$, and we can reasonably assume $\rho \ll 1$. We adopt the quasi-steady state assumption and approximate the number of droplets by

$$D = \frac{I}{\alpha}.$$

In addition, unless immunity is permanently acquired following infection, the duration of the immune period is small compared with the average human lifespan and $\phi \ll \psi$. We thus allow repopulation of the susceptible class solely through the loss of immunity and neglect the natural birth process, i.e. $\phi \approx 0$. The model reduces to two equations

$$\frac{dS}{dt} = \psi(1 - S - I) - \frac{R_0}{\alpha}IS, \tag{26}$$

$$\frac{dI}{dt} = \frac{R_0}{\alpha}IS - I, \tag{27}$$

with $\alpha = 1 + \alpha_1 \cos(\Omega t)$. In contrast to models with sinusoidal forcing applied directly to the transmission rate β, we find that the forcing appears in the denominator of the nonlinear term. Singularities are possible if $\alpha = 0$, however, a small forcing amplitude $\eta_1 \ll 1$ always yields $\alpha_1 \ll 1$ and division by zero is avoided.

3.2 Small-amplitude seasonal forcing

Equation (27) allows S to be written in terms of I as

$$S = \frac{\alpha(\dot{I} + I)}{R_0 I},$$

where the dot denotes the time derivative. This can be substituted into (26) to yield a single equation for I,

$$\alpha I \ddot{I} + \left[\dot{\alpha} I - \alpha \dot{I} + \alpha \psi I + R_0 I^2 \right] \dot{I} + I^2 \left[\dot{\alpha} - \psi R_0 + \psi R_0 I + R_0 I + \alpha \psi \right] = 0.$$

Assuming the seasonal forcing is small ($\alpha_1 \ll 1$), a perturbation $\xi(t)$ to the endemic equilibrium I_e such that

$$I \approx I_e + \alpha_1 \xi(t) = I_s(t),$$

satisfies the second order linear inhomogeneous equation

$$\frac{d^2 \xi}{dt^2} + (\psi + R_0 I_e) \frac{d\xi}{dt} + \psi(R_0 - 1)\xi = I_e \left[\Omega \sin(\Omega t) - \psi \cos(\Omega t) \right]. \tag{28}$$

The characteristic equation of the corresponding homogeneous problem is

$$\lambda^2 + (\psi + R_0 I_e)\lambda + \psi(R_0 - 1) = 0,$$

which has two negative roots $\lambda_{1,2} < 0$ given by

$$\lambda_{1,2} = \frac{-(\psi + I_e R_0) \pm \sqrt{(\psi - I_e R_0)^2 - 4 R_0 I_e}}{2}.$$

The solution of the inhomogeneous equation is then

$$\xi(t) = C_1 e^{-|\lambda_1| t} + C_2 e^{-|\lambda_2| t} + I_e \frac{\Omega[I_e R_0 - \Omega^2 - \psi^2] \sin(\Omega t) - I_e R_0 [\psi(\psi + 1) + \Omega^2] \cos(\Omega t)}{I_e^2 R_0^2 [(\psi + 1)^2 + \Omega^2] - 2 R_0 \Omega^2 I_e + \Omega^4 + \psi^2 \Omega^2},$$

$$\tag{29}$$

where C_1 and C_2 are arbitrary constants. At large times, $\xi(t)$ approaches a periodic solution with period Ω and amplitude

$$A = I_e\sqrt{\frac{\psi^2 + \Omega^2}{I_e^2 R_0^2[(\psi+1)^2 + \Omega^2] - 2R_0\Omega^2 I_e + \Omega^4 + \psi^2\Omega^2}}.$$

In addition, the solution for ξ has a phase Φ which will satisfy

$$\tan\Phi = \frac{I_e R_0(\psi^2 + \psi + \Omega^2)}{\Omega(\psi^2 + \Omega^2 - I_e R_0)}. \tag{30}$$

Thus, for small-amplitude seasonal forcing, the infected population can be approximated by

$$I_s(t) = I_e + \alpha_1 A \sin(\Omega t + \Phi). \tag{31}$$

Linear theory indicates that the infected population oscillates about the endemic state I_e with an amplitude $\alpha_1 A$. The period of oscillation is identical to that of the applied seasonal forcing and independent of the duration of acquired immunity. However, the disease incidence and seasonally forced pathogen inactivation are out of phase with each other. This is readily seen by rewriting (31) in the form

$$I_s(t) = I_e + \alpha_1 A \cos\left\{\Omega\left(t + \frac{2\Phi - \pi}{2\Omega}\right)\right\}, \tag{32}$$

and there is a time shift of $(2\Phi - \pi)/2\Omega$ between the two quantities, whereby $I_s(t)$ achieves its peak value before α does when $2\Phi - \pi > 0$. Furthermore, the maximum of $I_s(t)$ will not occur before the minimum of $\alpha(t)$ when

$$0 \leq \frac{2\Phi - \pi}{2\Omega} \leq \frac{\pi}{\Omega}. \tag{33}$$

Of course, a peak in α corresponds to the point of maximum pathogen inactivation and thus to a minimum in pathogen survival, and logically peak disease incidence should not coincide with minimal survival. Therefore, a more interesting and informative quantity is the delay

between minimum α (peak pathogen survival) and peak disease incidence. We denote this quantity as δ and find

$$\delta = \frac{3\pi - 2\Phi}{2\Omega}, \tag{34}$$

where Φ can be determined from (30). Thus, the extent of the observed delay between peak survival and peak incidence is determined from the specific disease parameters and the period of the seasonally forced inactivation rate.

Another consideration in the relative positions of the maximum incidence and inactivation is the time of pathogen introduction, corresponding to the time the first infected individual is introduced into the population. For example, pathogen introduction at the point of peak survival could have radically different dynamics to an introduction at the time of peak inactivation. To address the consequences of the introduction time we consider a seasonal variation of the form

$$\alpha(t) = 1 + \alpha_1 \cos\left[\Omega(t - t_0)\right], \tag{35}$$

and then investigate the dependence of our results on t_0. Equation (35) implies that the infected initial condition $I(t = 0)$ may be introduced at different points during the seasonal variation of the pathogen inactivation rate. Namely, the infected person(s) at $t = 0$ may be introduced in times that correspond to different pathogen inactivation rates. Given equation (35), the calculations were repeated, and we found that the time shift $t - t_0$ appears in the inhomogeneous term of the differential equation (28) and the infected population then satisfies

$$I_s(t) = I_e + \alpha_1 A \sin\left[\Omega(t - t_0) + \Phi\right],$$

which can be written as

$$I_s(t) = I_e + \alpha_1 A \cos\left\{\Omega\left(t - t_0 + \frac{2\Phi - \pi}{2\Omega}\right)\right\}. \tag{36}$$

It can then be easily shown that the delay δ does not depend on t_0, i.e. equation (34) remains valid, even for $t_0 \neq 0$. Therefore, we conclude that, while the solution of the

26

differential equation will invariably depend on the time of pathogen introduction, the delay between incidence $I(t)$ and inactivation $\alpha(t)$ does not.

3.3 The case of influenza

As discussed in Section 2.3, in the case of influenza we find $\phi \ll 1$ and it is reasonable to neglect the natural birth process. The values of the dimensionless parameters R_0, ρ and ψ are given by equation (20). The dimensionless frequency and amplitude are defined in (25). Assuming a seasonal forcing with a period of one year yields a frequency of $\Omega = 0.086$. Droplet removal through inhalation is negligible and θ can be approximated by the gravitational settling rate alone, for a 4μm droplet this yields $\theta = 28.8/$day (Robinson et al. 2012). The pathogen inactivation rate is assumed to be independent of droplet size and is taken to be $\eta_0 = 8.64/$day (Hemmes et al. 1960). Finally, assuming a value of $\eta_1 = 0.1$ for the forcing amplitude yields $\alpha_1 = 0.023$. In reality, the value of η_1 depends on the seasonal driver (e.g. temperature, humidity) and its related seasonal cycle. This work merely assumes that η_1 is small and the chosen value determines the amplitude of the forcing term and thus the amplitude of the disease incidence. It is clear from (31) that the delay and period of the linearised solution are not affected by the choice of η_1.

The disease incidence $I_s(t)$ will reach its maximum before the maximal viral inactivation $\alpha(t)$ provided $2\Phi - \pi > 0$. From (30), we calculate $\tan \Phi = 0.0167$, the inverse of which yields $\Phi_f = 0.0167$, where the subscript f indicates that this angle lies in the fundamental interval $[-\pi/2, \pi/2]$. However, the trigonometric coefficients in (29) are both negative and Φ must lie in the third quadrant, yielding $\Phi = 0.0167 + \pi$. It follows that $2\Phi - \pi = 3.175 > 0$. Furthermore, the relative positions of the incidence and inactivation curves can be further restricted, by requiring the satisfaction of (33), to ensure that the maximum of $I_s(t)$ will not occur before the minimum of $\alpha(t)$, and this condition reduces to

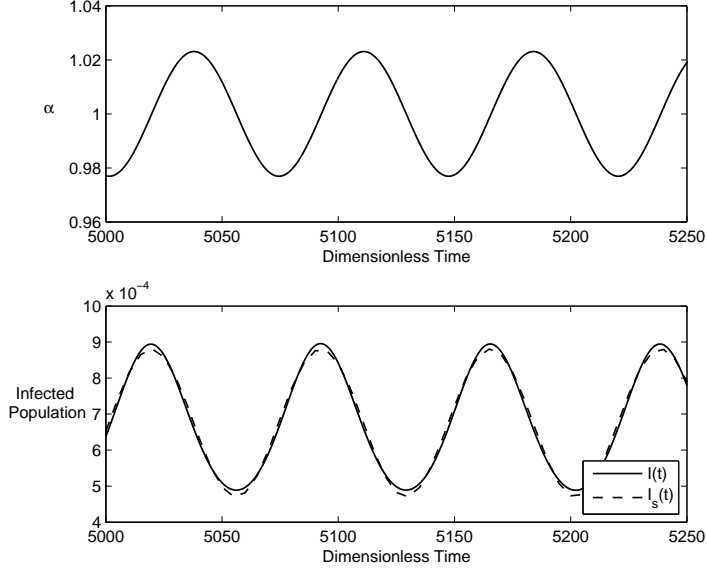$$\frac{\pi}{2} \leq \Phi \leq \frac{3\pi}{2} \implies -\frac{\pi}{2} \leq \Phi_f \leq \frac{\pi}{2},$$

Figure 7: Influenza seasonality with initial conditions $S(0) = 0.99$, $I(0) = 0.01$ and $D(0) = 10^{-3}$. Parameter values are $R_0 = 1.3$, $\rho \approx 0.005$, $\phi \approx 0.0002$, $\psi \approx 0.003$, $\Omega = 0.086$ and $\alpha_1 = 0.023$, with $t_0 = 0$.
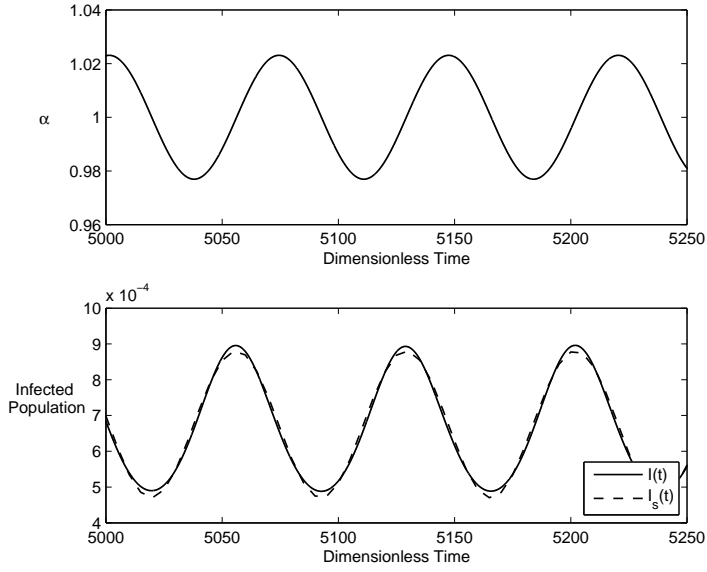

Figure 8: Influenza seasonality with initial conditions $S(0) = 0.99$, $I(0) = 0.01$ and $D(0) = 10^{-3}$. Parameter values are $R_0 = 1.3$, $\rho \approx 0.005$, $\phi \approx 0.0002$, $\psi \approx 0.003$, $\Omega = 0.086$ and $\alpha_1 = 0.023$, with $t_0 = \pi/\Omega$.

which is always satisfied by Φ_f.

A numerical solution of the dimensionless system (21)-(24), showing the pathogen inactivation $\alpha(t)$, the disease incidence $I(t)$ and the solution of the linearised system $I_s(t)$, is shown in Figure 7. The maximum disease incidence clearly occurs *before* maximum inactivation and *after* minimum inactivation. The time delay between peak virus survival (minimal α) and peak disease incidence is clearly visible and can be calculated from (34) as $\delta \approx 18.07$. Both curves, $I(t)$ and $\alpha(t)$, are observed to oscillate with the same period, as predicted by the linear analysis. The linearized quasi-steady solution $I_s(t)$, given by (36), provides a very good approximation to the solution of the full system. Figure 7 displays the disease incidence for the case $t_0 = 0$, such that the initial infected individual was introduced into the population at the point of maximum viral inactivation (minimum survival). To demonstrate the independence of the delay δ on the time of viral introduction, the simulation was re-run with the infected individual introduced at the point of minimum inactivation (maximum survival), i.e. $t_0 = \pi/\Omega$, Figure 8. The timing of peak disease incidence changes, however the predicted delay remains constant.

A numerical solution is shown in terms of dimensional variables in Figure 9, where it is assumed that the peak in disease incidence occurs in January and, for illustration purposes, we have fixed the total human population at 6 million. The solution indicates that disease incidence peaks approximately three months (≈ 90.33 days calculated from (34)) after the influenza virus inactivation reaches its minimum, at which time virus survival is at its peak. The magnitude of this delay is dependent on the disease parameters. The delay δ is plotted in dimensional form for varying R_0 in Figure 10(b). As R_0 increases the delay decreases and the disease incidence peak occurs earlier after the peak in influenza virus survival. The amplitude of the infectious wave as a function of R_0 is plotted in Figure 10(a). Clearly, amplitude increases with increasing R_0, indicating the occurrence of more severe outbreaks for large R_0 values.
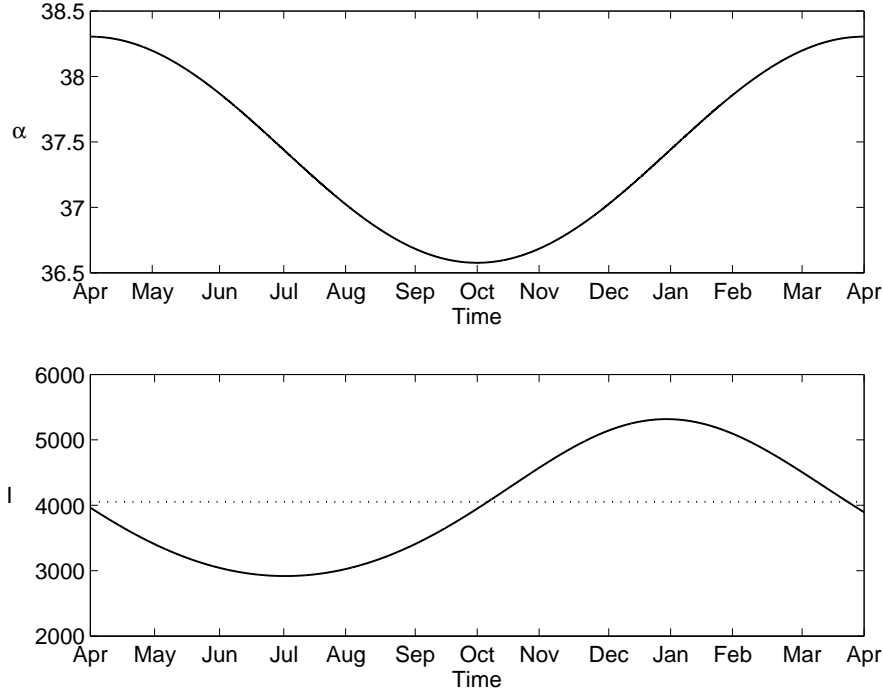
Figure 9: Numerical solution obtained with initial condition $S(0) = 0.99$, $I(0) = 0.01$ and $D(0) = 10^{-3}$. Parameter values $R_0 = 1.3$, $\rho \approx 0.005$, $\phi \approx 0.0002$, $\psi \approx 0.003$, $\Omega = 0.086$ and $\alpha_1 = 0.023$. All variables are dimensional.
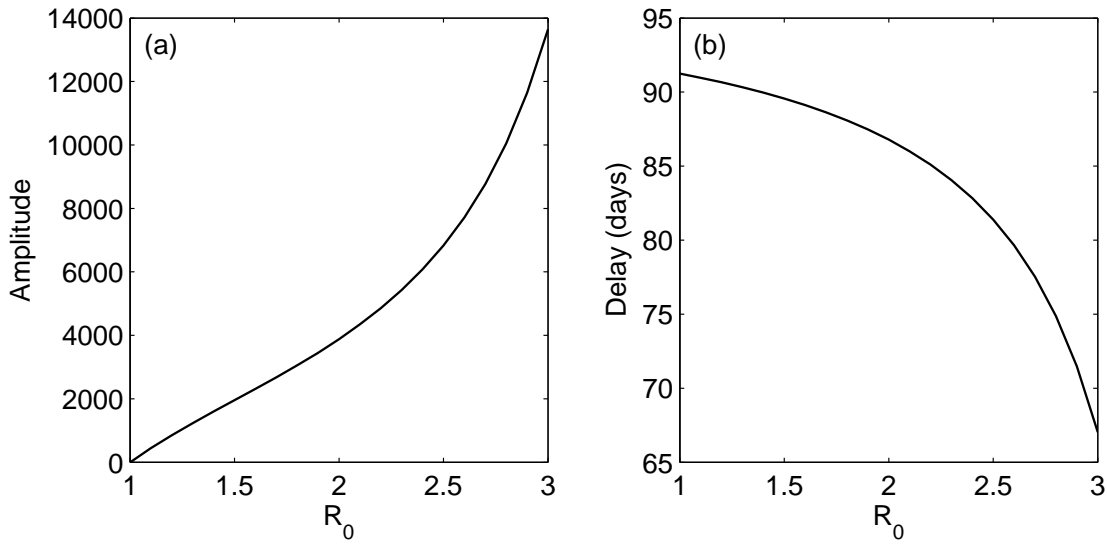

Figure 10: (a) Dimensional amplitude ($= N\alpha_1 A$) as a function of R_0 (b) Dimensional delay ($= \delta/(\mu + d)$) as a function of R_0. Parameter values $N = 6 \times 10^6$, $d = 4 \times 10^{-5}$/day, $\mu = 0.2$/day, $\theta = 28.8$/day $\eta_0 = 8.64$/day, $\eta_1 = 0.1$, $\omega = \frac{2\pi}{365}$.

4 Discussion

In this work we have presented a model for the transmission of an infectious disease by means of a pathogenic state capable of surviving in an environmental reservoir outside of its host organism. For a reproduction number exceeding unity, $R_0 > 1$, the pathogen dynamics are found to depend on the magnitude of a dimensionless number ρ, which represents the ratio between the pathogen lifespan and that of an infected individual. If the duration of the infectious disease state is significantly longer than the lifespan of the pathogen (e.g. for influenza), yielding $\rho \ll 1$, a rapid transient period is observed during which pathogen and infected numbers rapidly achieve a balance. Thereafter, the pathogen dynamics identically follow those of the infected population. At large times, the solution approaches a stable endemic disease state, exhibiting damped oscillations as it does so. In contrast, if the pathogen is capable of surviving significantly longer than the duration of the infectious disease state (e.g. cryptosporidium), yielding $\rho \gg 1$, the susceptible and infected populations first approach an intermediate state during which the pathogen number remains approximately constant. However, at large times all variables converge to a stable endemic state.

The effect of incorporating seasonal forcing through the pathogen inactivation rate was considered for the specific case of a respiratory infection mediated by airborne pathogen-loaded droplets. A quasi-steady state approximation allows the droplet dynamics to be neglected resulting in a classic SIRS model with the seasonal forcing appearing in the denominator of the transmission term. The assumption of small-amplitude seasonal forcing yields a linearized approximation to the infected population, given by (32). It was found that the infected population oscillates about the endemic disease state with an identical period to that of the seasonally forced pathogen inactivation rate and the period is independent of the duration of acquired immunity. In addition, the peak in pathogen survival (corresponding to minimal pathogen inactivation) was found to precede peak disease incidence. For the particular case of influenza with a reproduction number of $R_0 = 1.3$, this phase shift was calculated to be approximately three months, with shorter delays observed

31

for larger R_0 values, Figure 10.

A final topic worth noting in relation to the seasonal model presented in Section 3 is the interpretation of the basic reproduction number. In the seasonal context, this no longer corresponds to the average number of secondary infections per primary infection since this value will invariably be dependent on time. Attempts have been made to define R_0 in this context (Bacaër and Ait Dads 2012, Grassley and Fraser 2006) and the various attempts to derive a time-dependent expression have focused on the analysis of a time-dependent transmission term. However, in this work we attempt to tackle the issue of seasonality from a novel perspective by linking the seasonal signal to a palpable physical process. As such, the time-dependent R_0 would be intrinsically linked to the pathogen inactivation rate which is a complex function of environmental factors, which in turn are highly variable with geographic location. To this end, an elaboration on the issue of time-dependence is beyond the scope of this work.

The exact mechanism driving the seasonal occurrence of infectious diseases is uncertain. Several factors undoubtedly impact the dynamics, including human behavior and pathogen survival, and many of these factors are difficult to quantify. In particular, the burden placed on health systems by seasonal influenza, and the constant threat of deadly pandemics, makes understanding the transmission mechanisms of the virus an important issue. Experimental studies have identified the impact of environmental conditions on virus survival as a crucial factor. However, the primary sources of viral inactivation (temperature, humidity, solar radiation, etc.) have been difficult to identify, and indeed a complex combination of these sources working in unison is a likely culprit. More rigorous experimental work is needed to ascertain the primary source of the observed seasonality. Our model provides an insight into how annual variations in virus inactivation can influence disease incidence and the model is sufficiently general that it can be applied to various transmission pathways. A better understanding of pathogen removal processes could provide the opportunity to develop more complex models incorporating the effect and interaction of multiple environmental factors.

References

[1] Anderson, R.M., May, R.M., 1981. The population dynamics of microparasites and their invertebrate hosts. Phil. Trans. Roy. Soc. London B. 291, 451-524.

[2] Anderson, R.M., May, R.M., 1991. Infectious diseases in humans: dynamics and control. Oxford University Press.

[3] Atkinson, M.P., Wein, L.M., 2008. Quantifying the routes of transmission for pandemic influenza. Bull. Math. Biol. 70, 820-867.

[4] Bacaër, N., Ait Dads, E.H., 2012. On the biological interpretation of a definition for the parameter R_0 in periodic population models. J. Math. Biol. 65, 601-621.

[5] Bertuzzo, E., Casagrandi, R., Gatto, M., Rodriguez-Iturbe, I., Rinaldo, A., 2010. On spatially explicit models of cholera epidemics, J. R. Soc. Interface. 7, 321333.

[6] Burie, J.B., Calonnec, A., Ducrot, A., 2006. Singular perturbation analysis of travelling waves for a model in phytopathology. Math. Model. Nat. Phenom. 1, 49-62.

[7] Cannell, J.J., Zasloff, M., Garland, C.F., Scragg, R., Giovannucci, E., 2008. On the epidemiology of influenza. Virology Journal. 5, 29.

[8] Chowell, G., Miller, M.A., Viboud, C., 2008. Seasonal influenza in the United States, France and Australia: transmission and prospects for control. Epidemiol. Infect. 136, 852-864.

[9] Codeço, C.T., 2001. Endemic and epidemic dynamics of cholera: the role of the aquatic reservoir. BMC Infect. Dis. 1, 1.

[10] Cummings, J.H., Bingham, S.A., Heaton, K.W., Eastwood, M.A., 1992. Fecal weight, colon cancer risk, and dietary intake of nonstarch polysaccharides (dietary fiber). Gastroenterology. 103, 1783-1789.

[11] Dowell, S.F., 2001. Seasonal variation in host susceptibility and cycles of certain infectious diseases. Emerg. Infect. Dis. 7, 369-374.

[12] Dushoff, J., Plotkin, J.B., Levin, S.A., Earn, D.J.D., 2004. Dynamical resonance can account for seasonality of influenza epidemics. PNAS. 101, 16915-16916.

[13] Eisenberg, J.N., Seto, E.Y., Colford Jr, J.M., Olivieri, A., Spear, R.C., 1998. An analysis of the Milwaukee Cryptosporidiosis outbreak based on a dynamic model of the infection process. Epidemiology. 9, 255-263.

[14] Fisman, D.N., 2007. Seasonality of infectious diseases. Annu. Rev. Public Health. 28, 127-143.

[15] Glaberman, S., Moore, J.E., Lowery, C.J., Chalmers, R.M., Sulaiman, I., Elwin, K., Rooney, P.J., Millar, B.C., Dooley, J.S., Lal, A.A., Xiao, L., 2002. Three drinking-water associated Cryptosporidiosis outbreaks, Northern Ireland. Emerg. Infect. Dis. 8, 631-633.

[16] Grassly, N.C., Fraser, C., 2006. Seasonal infectious disease epidemiology. Proc. Roy. Soc. B. 273, 2541-2550.

[17] Harper, G.J., 1961. Airborne micro-organisms: survival tests with four viruses. J. Hyg. (Lond). 59, 479-486.

[18] Hemmes, J.H., Winkler, K.C., Kool, S.M., 1960. Virus survival as a seasonal factor in Influenza and Poliomyelitis. Nature. 188, 430-431.

[19] Joh, R.I., Wang, H., Weiss, H., Weitz, J.S., 2009. Dynamics of indirectly transmitted infectious diseasees with immunological threshold. Bull. Math. Biol. 71, 845-862.

[20] Keeling, M.J., Rohani, P., Grenfell, B.T., 2001. Seasonally forced disease dynamics explored as switching between attractors. Physica D. 148, 317-335.

[21] Li, S., Eisenberg, J.N.S., Spicknall, I.H., Koopman, J.S., 2009. Dynamics and control of infections transmitted from person to person through the environment. Am. J. Epidemiol. 170, 257-265.

[22] Lofgren, E., Fefferman, N.H., Naumov, Y.N., Gorski, J., Naumova, E.N., 2007. Influenza seasonality: underlying causes and modeling theories. J. Virol. 81, 5429-5436.

[23] Lowen, A.C., Mubareka, A., Steel, J., Palese, P., 2007. Influenza virus transmission is dependent on relative humidity and temperature. PLoS Pathogens. 3, 1470-1476.

[24] Medema, G., Teunis, P., Blokker, M., Deere, D., Charles, P., Loret, J.F., 2009. Risk assessment of Cryptosporidium in drinking water. World Health Organization.

[25] Miller, M.W., Thompson Hobbs, N., Tavener, S.J., 2006. Dynamics of prion disease transmission in mule deer. Ecological Applications. 16, 2208-2214.

[26] Nelson, R.J., Demas, G.E., 1996. Seasonal changes in immune function. Quart. Rev. Biol. 71, 511-548.

[27] Nicas, M., Nazaroff, W.W., Hubbard, A., 2005. Towards understanding the risk of secondary airborne infection: emission of respirable pathogens. J. Occup. Environ. Hyg. 2, 143-154.

[28] Nieuwhof, G.J., Conington, J., Bishop, S.C., 2009. A genetic epidemiological model to describe resistance to an endemic bacterial disease in livestock: application to footrot in sheep. Genetics Selection Evolution. 41, 19.

[29] Peeters, J.E., Mazás, E.A., Masschelein, W.J., Villacorta Martiez de Maturana, I., Debacker, E., 1989. Effect of disinfection of drinking water with ozone or chlorine dioxide on the survival of Cryptosporidium parvum oocysts. Appl. Environ. Microbiol. 55, 1519-1522.

[30] Reluga, T., 2004. A two-phase epidemic driven by diffusion. J. Theor. Biol. 229, 249-261.

[31] Robinson, M., Stilianakis, N.I., Drossinos, Y., 2012. Spatial dynamics of airborne infectious diseases. J. Theor. Biol. 297, 116-126.

[32] Schulman, J.L., Kilbourne, E.D., 1963. Experimental transmission of Influenza virus infection in mice II: some factors affecting the incidence of transmitted infection. J. Exp. Med. 118, 267-275.

[33] Shaman, J., Kohn, M., 2009. Absolute humidity modulates influenza survival, transmission, and seasonality. PNAS. 106, 3243-3248.

[34] Shaman, J., Pitzer, V.E., Viboud, C., Grenfell, B.T., Lipsitch, M., 2010. Absolute humidity and the seasonal onset of influenza in the continential United States. PLoS Biology. 8, e10000316.

[35] Stilianakis, N.I., Drossinos, Y., 2010. Dynamics of infectious disease transmission by inhalable respiratory droplets. J. Roy. Soc. Interface. 50, 1355-1366.

[36] Stohr, K., 2002. Influenza - WHO cares. Lancet Infect. Dis. 2, 517.

[37] Stone, L., Olinky, R., Huppert, A., 2007. Seasonal dynamics of recurrent epidemics. Nature. 446, 533-536.

[38] Tien, J.H., Earn, D.J.D., 2010. Multiple transmission pathways and disease dynamics in a waterborne pathogen model. Bull. Math. Biol. 72, 1506-1533.

[39] Truscott, J., Fraser, C., Cauchemez, S., Meeyai, A., Hinsley, W., Donnelly, C.A., Ghani, A., Ferguson, N., 2012. Essential epidemiological mechanisms underpinning the transmission dynamics of seasonal influenza. J. R. Soc. Interface. 67, 304-312.

[40] Weber, T.P., Stilianakis, N.I., 2008. Inactivation of influenza A viruses in the environment and modes of transmission: a critical review. J. Infect. 57, 361-373.

[41] Yang, Y., Sugimoto, J.D., Halloran, M.E., Basta, N.E., Chao, D.L., Matrajt, L., Potter, G., Kenah, E., Longini Jr, I.M, 2009. The transmissibility and control of pandemic influenza A (H1N1) virus. Science. 326, 729-733.